

A potential WIMP signature for the caustic ring halo model

Anne M. Green

*Astronomy Unit, School of Mathematical Sciences, Queen Mary University of London,
Mile End Road, London, E1 4NS, U. K.*

(December 2, 2024)

Weakly Interacting Massive Particle (WIMP) direct detection event rate calculations usually rely on fairly simple, essentially static, analytic halo models. This is largely since the resolution of numerical simulations not yet being large enough to allow the full numerical calculation of the WIMP density and velocity distribution. In this paper we study the direct detection rate, in particular its energy dependence and annual modulation, for the caustic ring halo model. In this model, which uses simple assumptions to model the infall of dark matter onto the halo, the distribution of the cold dark matter particles at the Earth's location has a series of peaks in velocity space. We find that the sign of the annual modulation in the event rate changes as a function of recoil energy, providing a potentially distinctive experimental signal. We then compare the theoretical predictions of this models with the experimental signal found by the DAMA experiment. We find that the DAMA data allow less than $\sim 30\%$ of the local halo density to be in the form of velocity flows.

PACS numbers: 98.70.V, 98.80.C

astro-ph/ddmmyy

I. INTRODUCTION

Weakly Interacting Massive Particle (WIMP) direct detection experiments are just reaching the sensitivity required to probe the interesting range of mass-cross section parameter space where relic neutralinos could constitute the dark matter. The DAMA collaboration, using a detector consisting of radiopure NaI crystal scintillators at the Gran Sasso Laboratory, have reported the detection of a 4σ annual modulation signal in their direct detection experiment, consistent with WIMP scattering [1,2]. Whilst this result is somewhat controversial [3,4] it illustrates the potential of current and upcoming WIMP direct detection experiments.

Event rate calculations and detection strategies for particle dark matter are usually based on the assumption of a standard Maxwellian halo model [5–7]. The standard Maxwellian halo model has a number of deficiencies, in particular the real halo contains substructure and is not perfectly spherical and isotropic [8]. Since the resolution of numerical simulations is not yet large enough to allow the full numerical calculation of the WIMP density and velocity distribution, analytic, or at least semi-analytic, models for the dark matter halo must be used. The direct detection rate and in particular its annual modulation, which occurs due to the Earth's motion, has been calculated for a range of analytic non-standard halo models [5,9–15]. It has been found that the region in the mass-cross section plane selected by the DAMA data depends substantially on the halo model assumed [10,12,15].

Analytic halo models usually assume an essentially static halo, whereas in reality the halo is forming via the ongoing infall of surrounding dark matter [16]. The caustic ring halo model, which arises from simple assumptions about the infall of dark matter onto the halo, provides an

analytic model of some features of the dark matter distribution which may result from this accretion process. It is therefore worthwhile to calculate the observational features which the caustic ring halo model produces. The directional WIMP direct detection rate, which would be probed by proposed experiments such as DRIFT [17], has been calculated by Copi, Han and Krauss [18], whilst Vergados [19] has calculated the total WIMP direct detection rate. In this paper we study the variation of the differential direct detection rate, in particular its annual modulation, with detector recoil energy.

II. CAUSTIC RING HALO MODEL

Cold dark matter (CDM) particles are collisionless and have low velocity dispersion ($< 30 \text{ km s}^{-1}$) so that particles falling onto an isolated galaxy are expected to oscillate in and out of the galaxy a number of times before they are virialised by inhomogeneities (such as molecular clouds, globular clusters and stars) [20]. These non-virialised CDM flows lead to the formation of caustic rings at the points where the particles with the most angular momentum in a given inflow reach their point of closest approach to the galactic centre, hence the name of the model. Furthermore the distribution of the particles at any given location is expected to have a series of peaks in velocity space, corresponding to particles which are falling into the galaxy for the first time and those which have fallen in and out a number of times but have not yet been thermalised. Whilst this model is obviously a simplification of the hierarchical accretion process via which the galactic halo forms, in particular the Milky Way is not an isolated galaxy, the resolution of N-body simulations is not yet large enough to resolve these sorts of features.

j	ρ_j (10^{-26} gcm $^{-3}$)	v_ϕ (kms $^{-1}$)	v_z (kms $^{-1}$)	v_r (kms $^{-1}$)
1	0.4	140	± 605	0
2	1.0	255	± 505	0
3	2.0	350	± 390	0
4	6.3	440	± 240	0
5	9.2	440	0	± 190
6	2.9	355	0	± 295
7	1.9	290	0	± 330
8	1.4	250	0	± 350
9	1.1	215	0	± 355
10	1.0	190	0	± 355
11	0.9	170	0	± 355
12	0.8	150	0	± 350
13	0.7	135	0	± 345
14	0.6	120	0	± 340
15	0.6	110	0	± 330
16	0.55	100	0	± 325
17	0.50	90	0	± 320
18	0.50	85	0	± 310
19	0.45	80	0	± 305
20	0.45	75	0	± 300

TABLE I. The density and velocity components, in the rest frame of the galaxy, of the velocity flows.

The velocities and densities at the Earth's location expected due to these flows have been calculated using the self-similar infall model [21] generalised to take into account the angular momentum of the CDM particles [22]. The Earth is located between the 4th and 5th caustic rings and the velocity flows corresponding to these two rings constitute roughly 30% of the local halo density. Analysis of 32 extended galactic rotation curves has provided some evidence for the 1st and 2nd caustic rings [23], whilst analysis of an IRAS map of the galactic disk apparently reveals the presence of the 5th ring [24].

The velocity distribution function of the velocity flows can be written as:

$$f(\mathbf{v}) = \Sigma_j \rho_j \delta(\mathbf{v} - \mathbf{v}_j), \quad (1)$$

where ρ_j and \mathbf{v}_j are the density and velocity of the j -th flow. Table I contains the most recently calculated values of ρ_j and \mathbf{v}_j [25] (note that there are two, inward and outward, flows for each velocity peak). The total density is $\rho_0 = 102$ gcm $^{-3} = 0.57$ GeVcm $^{-3}$, with the velocity flows contributing 65% of the total. We will assume that the thermalised background distribution is a Maxwellian with velocity dispersion $v_0 = 220$ kms $^{-1}$.

III. ANNUAL MODULATION SIGNAL

The WIMP detection rate depends on the speed distribution of the WIMPs in the rest frame of the detector, f_v . This is found from the halo velocity distribution, $f(\mathbf{v})$

by making a Galilean transformation $\mathbf{v} \rightarrow \tilde{\mathbf{v}} = \mathbf{v} - \mathbf{v}_e$, where \mathbf{v}_e is the Earth's velocity relative to the galactic rest frame, and then integrating over the angular distribution. In galactic co-ordinates the axis of the ecliptic lies very close to the $\phi - z$ plane and is inclined at an angle $\gamma \approx 29.80^\circ$ to the $\phi - r$ plane. Including all components of the Earth's motion, not just that parallel to the galactic rotation [11]:

$$\mathbf{v}_e = v_1 \sin \alpha \hat{r} + (v_0 + v_1 \cos \alpha \sin \gamma) \hat{\phi} - v_1 \cos \alpha \cos \gamma \hat{z}, \quad (2)$$

where $v_0 \approx 232$ kms $^{-1}$ is the speed of the sun with respect to the galactic rest frame, $v_1 \approx 30$ kms $^{-1}$ is the orbital speed of the Earth around the Sun and $\alpha = 2\pi(t - t_0)/T$, with $T = 1$ year and $t_0 \sim 153$ days (June 2nd), when the component of the Earth's velocity parallel to the Sun's motion is largest.

In the range of masses and interaction cross sections accessible to current direct detection experiments the best motivated WIMP candidate is the neutralino, for which the event rate is dominated by the scalar contribution. The differential event rate simplifies to (see e.g. Refs. [7,15] for details):

$$\frac{dR}{dE} = \xi \sigma_p \left[\frac{\rho_{0.3}}{\sqrt{\pi} v_0} \frac{(m_p + m_\chi)^2}{m_p^2 m_\chi^3} A^2 T(E) F^2(E) \right], \quad (3)$$

where it is conventional to normalise the local WIMP density, ρ_χ , to a fiducial value $\rho_{0.3} = 0.3$ GeVcm $^{-3}$, such that $\xi = \rho_\chi / \rho_{0.3}$, E is the energy deposited in the detector, A is the atomic number of the detector nuclei, $F(E)$ is the detector form factor (the Saxon Woods form factor is used for I whilst that of Na is taken to be unity, see e.g. Ref. [10]) and $T(E)$ is defined as [7]

$$T(E) = \frac{\sqrt{\pi} v_0}{2} \int_{v_{\min}}^{\infty} \frac{f_v}{v} dv, \quad (4)$$

where v_{\min} is the minimum detectable WIMP velocity

$$v_{\min} = \left(\frac{E(m_\chi + m_A)^2}{2m_\chi^2 m_A} \right)^{1/2}, \quad (5)$$

m_χ is the WIMP mass and m_A is the atomic mass of the target nuclei.

In order to compare the theoretical signal with that observed we need to take into account the response of the detector. The electron equivalent energy, E_{ee} , which is actually measured is a fixed fraction of the recoil energy: $E_{ee} = q_A E$. The quenching factors for I and Na are $q_I = 0.09$ and $q_{Na} = 0.30$ respectively [26]. The energy resolution of the detector [9] is already taken into account in the data released by the DAMA collaboration.

The expected experimental spectrum per energy bin for the DAMA collaboration set-up is then given by [10]

j	ρ_j (10^{-26} gcm $^{-3}$)	v_ϕ (kms $^{-1}$)	\tilde{v}_ϕ (kms $^{-1}$)	\tilde{v}_{tot} (kms $^{-1}$)
1	0.4	140	-104 (-78)	609 (605)
2	1.0	255	11 (37)	505 (506)
3	2.0	350	106 (132)	409 (416)
4	6.3	440	196 (222)	310 (327)
5	9.2	440	196 (222)	273 (292)
6	2.9	355	111 (137)	311 (321)
7	1.9	290	46 (72)	333 (338)
8	1.4	250	6 (32)	350 (351)
9	1.1	215	-29 (-3)	356 (355)
10	1.0	190	-54 (-28)	359 (356)
11	0.9	170	-74 (-48)	363 (358)
12	0.8	150	-94 (-68)	362 (357)
13	0.7	135	-109 (-83)	362 (355)
14	0.6	120	-124 (-98)	362 (354)
15	0.6	110	-134 (-108)	356 (347)
16	0.55	100	-144 (-118)	355 (346)
17	0.50	90	-154 (-128)	355 (345)
18	0.50	85	-159 (-133)	348 (337)
19	0.45	80	-164 (-138)	346 (335)
20	0.45	75	-169 (-143)	344 (332)

TABLE II. The density, ϕ velocity component in the rest frame of the galaxy v_ϕ , ϕ velocity component in the rest frame of the Earth \tilde{v}_ϕ , and total speed in the rest frame of the Earth \tilde{v}_{tot} , of the caustic flows in June, when $\alpha = 0$ (and in December when $\alpha = \pi$).

$$\frac{\Delta R}{\Delta E}(E) = r_{\text{Na}} \int_{E/q_{\text{Na}}}^{(E+\Delta E)/q_{\text{Na}}} \frac{dR_{\text{Na}}}{dE_{\text{ee}}}(E_{\text{ee}}) \frac{dE_{\text{ee}}}{\Delta E} + r_{\text{I}} \int_{E/q_{\text{I}}}^{(E+\Delta E)/q_{\text{I}}} \frac{dR_{\text{I}}}{dE_{\text{ee}}}(E_{\text{ee}}) \frac{dE_{\text{ee}}}{\Delta E}, \quad (6)$$

where $r_{\text{Na}} = 0.153$ and $r_{\text{I}} = 0.847$ are the mass fractions of Na and I respectively. Since $v_0 \gg v_1$ the differential event rate in the k -th energy bin can be expanded in a Taylor series in $\cos \alpha$ [6]:

$$\frac{\Delta R}{\Delta E}(E_k) \approx S_{0,k} + S_{m,k} \cos \alpha. \quad (7)$$

IV. RESULTS

Whilst all 3 components of the Earth's velocity need to be included to calculate the annual modulation signal accurately, the signal is largely determined by the component in the galactic plane [6]:

$$v_{e,\phi} = v_{\text{circ}} [1.05 + 0.06 \cos \alpha], \quad (8)$$

where $v_{\text{circ}} = 220$ kms $^{-1}$ is the local circular velocity about the galactic centre. Before presenting the results of a numerical calculation, using all three components of the Earth's velocity we will carry out a simple analytic calculation, using only the component in the galactic plane,

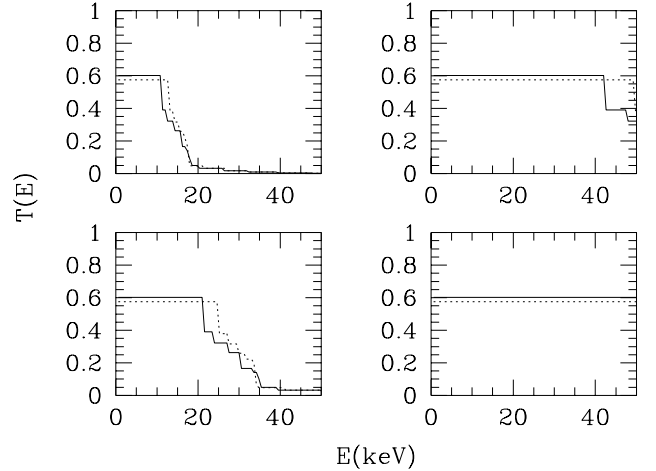


FIG. 1. The value of $T(E)$ in June (solid line) and December (dotted line) due to the velocity flows alone for four values of the WIMP mass $m_\chi = 30, 50, 100, 200$ GeV, (top left, bottom left, top right and bottom right respectively).

in order to elucidate the physical origin of the variation in $T(E)$.

In June when $\alpha = 0$

$$v_{e,\phi} = 1.11 \times v_\odot = 244.2 \text{ kms}^{-1}, \quad (9)$$

whilst in December when $\alpha = \pi$

$$v_{e,\phi} = 0.99 \times v_\odot = 217.8 \text{ kms}^{-1}. \quad (10)$$

Table 2 contains the density, ϕ -velocity component, in the rest frames of the galaxy and Earth, and the total velocity in the rest frame of the Earth of the velocity flows for $\alpha = 0$ and π . In both cases the total density in flows with negative v_ϕ (incident from the forward direction) is 17.1×10^{-26} gcm $^{-3}$ whilst the total density in flows with positive v_ϕ (incident from the backward direction) is 49.4×10^{-26} gcm $^{-3}$ i.e. there are more WIMPs incident from backwards than forwards as found by Copi, Han and Krauss [18]. This is the opposite of the directional signal produced by a pure Maxwellian halo.

In order to illustrate how the variations due to the caustics are smoothed out by the isothermal background we plot $T(E)$, as a function of E , for a Ge 76 detector in Fig. 1 for the velocity flows alone, and in Fig. 2 for the complete halo model described above in Sec. II, where the velocity flows contribute 65% of the local density with the remaining 35% in an isothermal background. Values for other monatomic detectors can be found by rescaling the x-axis by $m_A/(m_A + m_\chi)^2$.

For a pure Maxwellian halo the signal is largest in December for small recoil energies, switching to become largest in June as the recoil energy is increased [13]. The signal for the velocity flows alone is more complicated. The contribution of the j -th velocity flow to $T(E)$ is proportional to $\rho_j/\tilde{v}_{\text{tot}}$ if $\tilde{v}_{\text{tot}} > v_{\text{min}}$ and is zero otherwise. The contribution of the high density flows to the signal

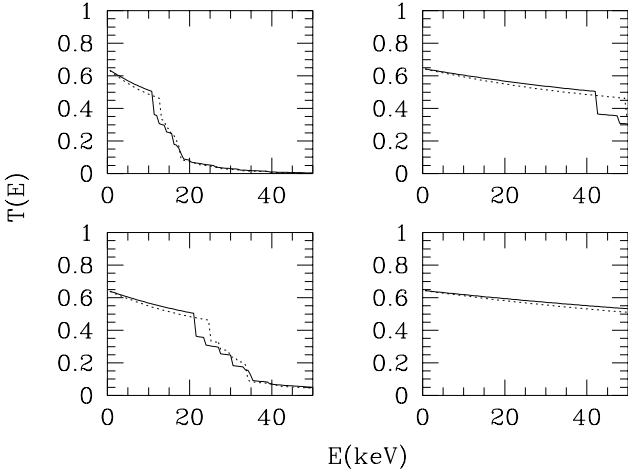


FIG. 2. The value of $T(E)$ in June (solid line) and December (dotted line) for a halo model with caustics plus an isothermal background, for four values of the WIMP mass $m_\chi = 30, 50, 100, 200$ GeV, (as before).

is largest in June, since their \tilde{v}_{tot} is smaller in June than in December. Therefore at low energies, where all the velocity flows contribute to the signal, the signal is largest in June. A given high density velocity flow stops contributing to the signal, $\tilde{v}_{\text{tot}} < v_{\text{min}}$, for smaller v_{min} , or equivalently E , in June compared to December however. This means that the steplike decreases in $T(E)$, which arise when a given flow stops contributing to the signal, occur at lower energies in June than in September (see Fig. 1). In other words for some range of recoil energies a given flow contributes to the signal in December but not in June. At large recoil energies only the low density flows, with high total velocity, can contribute and consequently the signal is far smaller than at low recoil energies. The lower density flows have negative \tilde{v}_ϕ and, in contrast to the high density flows, have larger speeds in June than in December, so that at high recoil energies the contribution due to a given flow is slightly larger in December. As m_χ is increased the variations in $T(E)$ are moved to higher E . The presence of a Maxwellian background smoothes the stepped variations in the signal produced by the flows, but they are still discernible and if detected would provide a distinctive indication of the presence of velocity flows.

In Fig. 3 we plot the differential event rate, dR/dE , for the velocity flows plus isothermal background model and also for a pure Maxwellian halo, for a NaI detector using the best fit values of the WIMP mass and cross-section found by the DAMA collaboration, $m_\chi = 54$ GeV $\xi\sigma_p = 4 \times 10^{-6}$ pb.

Brhlik and Roszkowski [10] have devised a technique for comparing the experimental results released by DAMA with theoretical predictions for the annual modulation signal, in the absence of detailed information about the experimental set-up, such as the efficiency of each NaI crystal. They define a function κ :

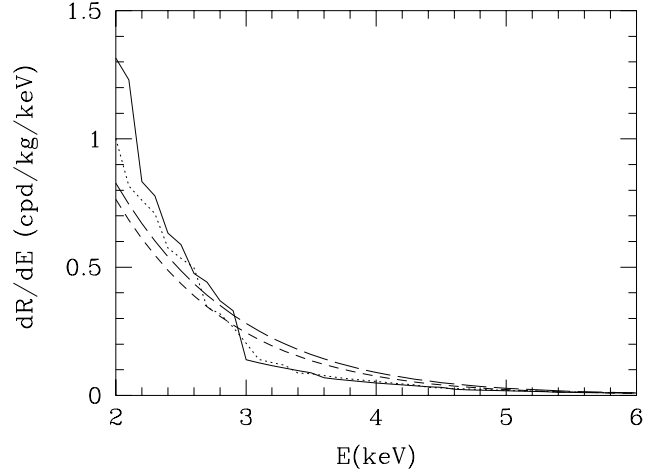


FIG. 3. The differential event rate dR/dE in June (solid line) and December (dotted line) for the caustic ring halo model with velocity flows plus a Maxwellian background as described in the text, and for a pure Maxwellian halo (June-long dashed line, December-short dashed line), for WIMP mass $m_\chi = 54$ GeV and cross-section $\xi\sigma_p = 4 \times 10^{-6}$ pb, as found by the DAMA collaboration, for a NaI detector.

Energy (keV)	$S_{0,k}$ (cpd/kg/keV)	$S_{m,k}$ (cpd/kg/keV)
2-3	0.54 ± 0.09	0.023 ± 0.006
3-4	0.21 ± 0.05	0.013 ± 0.002
4-5	0.08 ± 0.02	0.007 ± 0.001
5-6	0.03 ± 0.01	0.003 ± 0.001

TABLE III. $S_{0,k}$ and $S_{m,k}$ values obtained, by the DAMA collaboration, from a maximum likelihood analysis of their combined data from four annual cycles.

$$\kappa = \sum_k \frac{(S_{0,k}^{\text{th}} - S_{0,k}^{\text{exp}})^2}{\sigma_{0,k}^2} + \sum_k \frac{(S_{m,k}^{\text{th}} - S_{m,k}^{\text{exp}})^2}{\sigma_{m,k}^2}, \quad (11)$$

where the experimental errors on the time dependent and independent parts of the signal, found by the DAMA collaboration via a maximum likelihood analysis, $\sigma_{m,k}$ and $\sigma_{0,k}$ respectively, serve as weights. The values of $S_{0,k}$ and $S_{m,k}$, and the errors on them, found by DAMA for each energy bin [2] are reproduced in Table 3.

The contour, in the $m_\chi - \xi\sigma_p$ plane, $\kappa = 35$ agrees reasonably well with the DAMA collaborations' 3σ contour. Whilst this approach does not give accurate confidence limits on m_χ and $\xi\sigma_p$ it does a good job of reproducing the shape of the likelihood contours produced via a full likelihood analysis of the data [15].

To illustrate how the allowed region, in the $m_\chi - \xi\sigma$ plane, changes as the fraction of the local density in velocity flows is increased, in Fig. 4 we plot the $\kappa = 35$ contour for a pure Maxwellian halo and for models with velocity flows making up 10% and 20% of the local density, with the remainder in a Maxwellian background. The total local density in each case is taken to be $\rho_0 = 0.57$ GeVcm⁻³

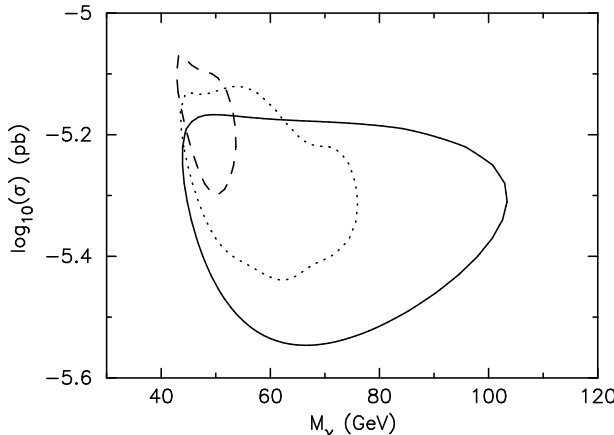


FIG. 4. The $\kappa = 35$ contour, delineating the region of $m_\chi - \xi\sigma$ parameter space compatible with the DAMA annual modulation signal, for a pure Maxwellian halo (solid line) and for a model with velocity flows making up 10% and 20% (dotted and dashed lines) of the local density with the remainder in a Maxwellian background. The total local density is taken to be $\rho_0 = 0.57 \text{ GeV cm}^{-3}$.

as above, although contours for other values of the local density can be found by simply rescaling the y-axis.

Brhlik and Roszkowski [10] found that, for a pure Maxwellian halo, the cut-off at large WIMP masses in the allowed region is determined by the time-dependent part of the signal (i.e. $S_{m,k}^{\text{th}}$), whilst the lower limit on the WIMP mass depends on both the time independent and dependent parts of the signal. When a velocity flow component is added to the Maxwellian background the time-independent part of the signal falls off less rapidly with increasing recoil energy for large WIMP masses (see Figs. 2 and 3) and this leads to the large mass cut-off in the allowed region moving to smaller masses. For smaller WIMP masses ($40 < M_\chi < 75 \text{ GeV}$) the time-dependent part of the signal is slightly larger, whilst the time-independent part is significantly smaller, compared to the signal produced by a pure Maxwellian. The combined result of these effects is that the allowed region is reduced in size and shifted to larger cross-sections and smaller masses. If more than $\sim 30\%$ of the local density is in the form of velocity flows then the allowed region disappears completely. The ‘wiggles’ in the boundary of the allowed region are a genuine effect and not an artifact of grid spacing or smoothing; as the WIMP mass is increased the recoil energy at which a given velocity flow stops contributing to the signal is increased leading to, non-synchronous, jumps in both the time dependent and independent parts of the signal.

We have found, using Brhlik and Roszkowskis’ analysis technique, that the DAMA data are not compatible with more than $\sim 30\%$ of the local density being in velocity flows. A full likelihood analysis of the raw data would be required to produce a precise limit. It should also be borne in mind that confirmation of the DAMA result from other experiments is, as yet, awaited. None

the less this analysis illustrates that constraints on the local structure of the galactic halo can potentially be derived even from the current generation of WIMP direct detection experiments.

V. CONCLUSIONS

In this paper we have studied the WIMP direct detection signal, in particular its annual modulation, for the caustic ring halo model. In this model the WIMP distribution at the Earth’s location has a series of peaks in velocity space, corresponding to particles which are falling into the galaxy for the first time and those which have fallen in and out a number of times but have not yet been thermalised. These peaks produce a distinctive imprint in the differential event rate, with the sign of the annual modulation (i.e. whether the event rate is larger in June or December) changing with detector recoil energy. The presence of an isothermal background component to the halo smoothes out the sharp changes in the differential event rate produced by the velocity flows but the distinctive changes in the sign of the annual modulation remain potentially discernible.

Finally we compared the predictions of the caustic ring halo model with the DAMA annual modulation data. The DAMA data are not compatible with more than $\sim 30\%$ of the local density being in velocity flows. Whilst the validity of this data is at present a matter of debate, our analysis illustrates that constraints on the local structure of the galactic halo can potentially be derived even using the current generation of WIMP direct detection experiments. Furthermore this suggests that if a significant component of the galactic dark matter is composed of WIMPs, then WIMP direct detection experiments with fine grained directional and energy resolution may be able to probe the local galactic structure, complementing the information which indirect detection experiments [27] would be able to provide on larger scales.

ACKNOWLEDGEMENTS

A.M.G. was supported by PPARC and acknowledges use of the Starlink computer system at QMW. A.M.G thanks Craig Copi, Simon Goodwin and especially Pierre Sikivie for useful discussions.

- [1] R. Bernabei et. al. Phys. Lett. **B389**, 757 (1996); ibid **B408**, 439 (1997); ibid **B424**, 195 (1998); ibid **B450**, 448 (1999).
- [2] R. Bernabei et. al. Phys. Lett. **B480**, 23 (2000).

- [3] G. Gerbier, J. Mallet, L. Mosca and C. Tao, astro-ph/9710181; astro-ph/9902194.
- [4] CDMS Collaboration, Nucl. Instrum. Meth. **A444** 345 (2000); Phys. Rev. Lett. **84**, 5699 (2000).
- [5] A. K. Drukier, K. Freese and D. N. Spergel, Phys. Rev. D **33**, 3495 (1986).
- [6] K. Freese, J. Frieman and A. Gould, Phys. Rev. D **37**, 3388 (1988).
- [7] G. Jungman, M. Kamionkowski and K. Griest, Phys. Rep. 267, 195 (1996).
- [8] J. F. Navarro, C. S. Frenk and S. D. M. White, Astophys. J. **462**, 563 (1996); B. Moore et. al. Mon. Not. R. Astron. Soc. **310** (1999), 1147; A. V. Kravtsov et. al. Astrophys. J. **502**, 48 (1998).
- [9] F. Donato, N. Fornengo and S. Scopel, Astropart. Phys. **9**, 247 (1998).
- [10] M. Brhlik and L. Roszkowski, Phys. Lett. **B464**, 303 (1999).
- [11] J. D. Vergados, Phys. Rev. Lett. **83**, 3597 (1999); Phys. Rev. D **62**, 023519 (2000).
- [12] P. Belli et. al. Phys. Rev. D **61**, 023512 (2000).
- [13] P. Ullio and M. Kamionkowski, hep-ph/0006183.
- [14] N. W. Evans, C. M. Carollo and P. T. de Zeeuw, astro-ph/0008156.
- [15] A. M. Green, to appear in Phys. Rev. D, astro-ph/0008138.
- [16] J. E. Gunn and J. R. Gott, ApJ **176**, 1 (1972).
- [17] M. Lehner et. al., astro-ph/9905074, proceedings of '2nd International Conference on Dark Matter in Astro and Particle Physics', Heidelberg 1998, 767-771.
- [18] C. J. Copi, J. Heo and L. M. Krauss, Phys. Lett. **B461**, 43 (1999); C. J. Copi and L. M. Krauss, astro-ph/0009467.
- [19] J. D. Vergados, hep-ph/0010151 to appear in the proceedings of 'NANPino-2000, Non Accelerator New Physics in Neutrino Observations', Dubna, Russia.
- [20] J. R. Ipser and P. Sikivie, Phys. Lett. B **291**, 288 (1992).
- [21] J. A. Filmore and P. Goldreich, ApJ **281** 1 (1984); E. Bertschinger, ApJ Suppl. **58**, 39 (1985).
- [22] P. Sikivie, I. I. Tkachev and Y. Wang, Phys. Rev. Lett. **75**, 2911 (1995); Phys. Rev. D **56**, 1863 (1997).
- [23] W. H. Kinney and P. Sikivie, Phys. Rev. D **61**, 087305 (2000).
- [24] P. Sikivie, private communication.
- [25] P. Sikivie, Nucl. Phys. Proc. Suppl. **72**, 110 (1999).
- [26] K. Fushimi et. al. Phys. Rev. C **47**, R245 (1993); G. J. Davies et. al. Phys. Lett. **B322**, 159 (1994); P. F. Smith et. al. Phys. Lett. **B379**, 299 (1996).
- [27] C. Calcareo-Roldan and B. Moore, Phys. Rev. D **62**, 123005 (2000); L. Bergström, J. Edsjö and C. Gunnarsson, astro-ph/001346.